Applied Physics Letters

RESEARCH ARTICLE | AUGUST 22 2022

Determining Young's modulus via the eigenmode spectrum of a nanomechanical string resonator

Yannick S. Klaß ; Juliane Doster ; Maximilian Bückle; Rémy Braive ; Eva M. Weig

Appl. Phys. Lett. 121, 083501 (2022)
https://doi.org/10.1063/5.0100405

AIP Publishing

Applied Physics Letters ARTICLE scitation.org/journal/apl

Determining Young's modulus via the eigenmode spectrum of a nanomechanical string resonator

Cite as: Appl. Phys. Lett. **121**, 083501 (2022); doi: 10.1063/5.0100405
Submitted: 24 May 2022 · Accepted: 4 August 2022 ·
Published Online: 22 August 2022

Yannick S. Klaß,[1,2] Juliane Doster,[2] Maximilian Bückle,[2] Rémy Braive,[3,4] and Eva M. Weig[1,2,5,6,a)]

AFFILIATIONS

[1]Department of Electrical and Computer Engineering, Technical University of Munich, 85748 Garching, Germany
[2]Department of Physics, University of Konstanz, 78457 Konstanz, Germany
[3]Centre de Nanosciences et de Nanotechnologies, CNRS, Université Paris-Sud, Université Paris-Saclay, 91767 Palaiseau, France
[4]Université de Paris, 75207 Paris Cedex 13, France
[5]Munich Center for Quantum Science and Technology (MCQST), 80799 Munich, Germany
[6]TUM Center for Quantum Engineering (ZQE), 85748 Garching, Germany

[a)]**Author to whom correspondence should be addressed:** eva.weig@tum.de

ABSTRACT

We present a method for the *in situ* determination of Young's modulus of a nanomechanical string resonator subjected to tensile stress. It relies on measuring a large number of harmonic eigenmodes and allows us to access Young's modulus even for the case of a stress-dominated frequency response. We use the proposed framework to obtain Young's modulus of four different wafer materials, comprising three different material platforms amorphous silicon nitride, crystalline silicon carbide, and crystalline indium gallium phosphide. The resulting values are compared with theoretical and literature values where available, revealing the need to measure Young's modulus on the sample material under investigation for precise device characterization.

Young's modulus of a material determines its stiffness under uniaxial loading. It is, thus, a crucial material parameter for many applications involving mechanical or acoustic degrees of freedom, including nano- and micromechanical systems,[1] cavity optomechanics,[2] surface or bulk acoustic waves, including quantum acoustics,[3,4] nanophononics,[5] or solid-state-based spin mechanics,[6] just to name a few. For quantitative prediction or characterization of the performance of those devices, precise knowledge of Young's modulus is required. This is particularly important, as the value of Young's modulus of most materials has been known to strongly depend on growth and even nanofabrication conditions such that relying on literature values may lead to significant deviations.[7–10] This is apparent from Fig. 1 where we show examples of experimentally and theoretically determined values of Young's modulus along with common literature values for three different material platforms. For amorphous stoichiometric Si_3N_4 grown by low pressure chemical vapor deposition (LPCVD), for instance, experimental values between 160[11] and 370 GPa[12] have been reported. The situation is considerably more complex for crystalline materials, for which additional parameters such as the crystal direction or, in the case of polymorphism or polytypism, even the specific crystal structure, affect the elastic properties. For these materials, Young's modulus can, in principle, be calculated via the elastic constants of the crystal.[13] However, its determination may be impeded by the lack of literature values of the elastic constants for the crystal structure under investigation, such that the database for theoretical values is scarce. This is seen for the ternary semiconductor alloy $In_{1-x}Ga_xP$, where even the gallium content x influences Young's modulus.[13] For 3C–SiC, another crystalline material, theoretical predictions vary between 125[14] and 466 GPa,[15] even surpassing the spread of experimentally determined values, because the literature provides differing values of the elastic constants. The apparent spread of the reported values clearly calls for reliable local and *in situ* characterization methods applicable to individual devices.

While Young's modulus of macroscopic bulk or thin film samples is conveniently characterized using ultrasonic methods[16,17] or static techniques such as nanoindentation,[18] load deflection,[12,19] or bulge testing,[20–22] determining its value on a nanostructure is far from trivial. For freely suspended nanobeams and cantilevers, a dynamical characterization via the eigenfrequency provides reliable results.[7,8,23–25] However, this method fails for nanomechanical devices such as membranes or strings subject to a strong intrinsic tensile prestress, where

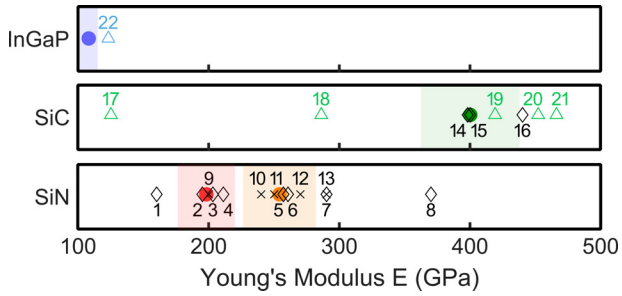

FIG. 1. Young's modulus for $In_{0.415}Ga_{0.585}P$, 3C–SiC, and LPCVD Si_3N_4. Our measured values and uncertainties are shown as filled colored circles and colored shades, respectively, whereas literature values are represented as open symbols. Colored open triangles correspond to values computed form literature values of the elastic constants, matching the crystal direction of the investigated resonators. Measured and other literature values are shown as open black diamonds and crosses, respectively. For the sake of visibility, we omit all stated uncertainties. Values are taken from: 1,[11] 2,[16] 3,[19] 4,[25] 5,[20] 6,[23] 7,[21] 8,[12] 9,[32] 10,[33] 11,[31,34] 12,[30] 13,[35] 14,[22] 15,[18] 16,[10] 17,[14] 18,[36] 19,[37] 20,[38] 21,[15] and 22.[13] Labels for measured values are found below the corresponding symbol, while all other labels are situated above.

the contribution of the bending rigidity and, thus, Young's modulus to the eigenfrequency becomes negligible. Given the continuously increasing interest in this type of materials resulting from the remarkably high mechanical quality factors of several 100 000 at room temperature[25–27] arising from dissipation dilution,[11,28,29] which can be boosted into the millions by soft clamping and further advanced concepts,[30,31] this calls for an accurate method to determine Young's modulus of stressed nanomechanical resonators.

Here, we present a method for *in situ* determination of Young's modulus of nanomechanical string resonators. It is based on the Euler–Bernoulli beam theory and relies on the experimental characterization of a large number of harmonic eigenmodes, which enables us to extract the influence of the bending rigidity on the eigenfrequency despite its minor contribution. We showcase the proposed method to determine the respective Young's modulus of four different wafers, covering all three material platforms outlined in Fig. 1.

According to the Euler–Bernoulli beam theory, the out-of-plane flexural eigenfrequencies of a doubly clamped string subjected to tensile stress with simply supported boundary conditions are calculated as[39,40]

$$f_n = \frac{n^2\pi}{2L^2}\sqrt{\frac{Eh^2}{12\rho}+\frac{\sigma L^2}{n^2\pi^2\rho}}, \tag{1}$$

where n is the mode number, L is the length, h is the thickness of the resonator, ρ is the density, E is Young's modulus, and σ is the tensile stress. For the case of strongly stressed nanostrings, the bending contribution to the eigenfrequency, i.e., the first term under the square root, will only have a minor contribution compared to the significantly larger stress term. Hence, the eigenfrequency-vs-mode number diagram will approximate the linear behavior of a vibrating string, $f_n \approx (n/2L)\sqrt{\sigma/\rho}$. So even for a large number of measured harmonic eigenmodes, only minute deviations from linear behavior imply that Young's modulus can only be extracted with large uncertainty. However, computing f_n^2/n^2 for two different mode numbers and subtracting them from each other allows it to cancel the stress term from the equation, yielding

$$\frac{f_n^2}{n^2}-\frac{f_m^2}{m^2} = E\frac{\pi^2h^2(n^2-m^2)}{48L^4\rho}, \tag{2}$$

with $m \neq n$. This equation can be solved for Young's modulus

$$E = \frac{48L^4\rho}{\pi^2h^2(n^2-m^2)}\cdot\left(\frac{f_n^2}{n^2}-\frac{f_m^2}{m^2}\right), \tag{3}$$

which allows us to determine Young's modulus from just the basic dimensions of the string resonator, the density, and the measured eigenfrequency of two different modes.

The associated uncertainty δE obtained by propagation of the uncertainties of all parameters entering Eq. (3) is discussed in the supplementary material. We show that the uncertainty of the density, the thickness, and the length of the string lead to a constant contribution to δE, which does not depend on the mode numbers n and m. The uncertainty of the eigenfrequencies, however, is minimized for high mode numbers and a large difference between n and m. Therefore, it is indispensable to experimentally probe a large number of harmonic eigenmodes to enable a precise result for Young's modulus.

To validate the proposed method, we are analyzing samples fabricated from four different wafers on three material platforms outlined in Fig. 1. Two wafers consist of 100 nm LPCVD-grown amorphous stoichiometric Si_3N_4 on a fused silica substrate (denoted as SiN-FS) and on a sacrificial layer of SiO_2 atop a silicon substrate (SiN-Si). The third wafer hosts 110 nm of epitaxially grown crystalline 3C–SiC on a Si(111) substrate (denoted as SiC). The fourth wafer comprises a 100 nm thick $In_{0.415}Ga_{0.585}P$ film epitaxially grown atop a sacrificial layer of $Al_{0.85}Ga_{0.15}As$ on a GaAs wafer (denoted as InGaP). All four resonator materials exhibit a substantial amount of intrinsic tensile prestress. Details regarding the wafers are listed in the supplementary material.

On all four wafers, we fabricate a series of nanostring resonators with lengths spanning from 10 to 110 μm in steps of 10 μm as shown in Fig. 2. However, as the tensile stress has shown to depend on the length of the nanostring in a previous work[41] and might have an

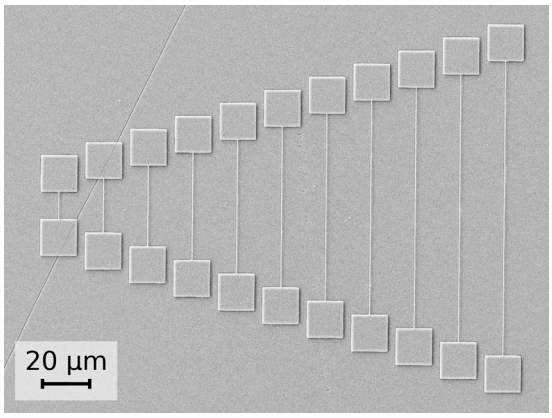

FIG. 2. Scanning electron micrograph of a series of nanostring resonators with lengths increasing from 10 to 110 μm in steps of 10 μm.

impact of Young's modulus,[42] we focus solely on the three longest strings of each sample for which the tensile stress has converged to a constant value[41] (see the supplementary material for a comparison of Young's modulus of all string lengths).

For each resonator, we determine the frequency response for a series of higher harmonics by using piezoactuation and optical interferometric detection. The drive strength is adjusted to make sure to remain in the linear response regime of each mode. The interferometer operates at a wavelength of 1550 nm and is attenuated to operate at the minimal laser power required to obtain a good signal-to-noise ratio to avoid unwanted eigenfrequency shifts caused by absorption-induced heating of the device. This is particularly important as the position of the laser spot has to be adapted to appropriately capture all even and odd harmonic eigenmodes. We extract the resonance frequencies by fitting each mode with a Lorentzian function as visualized in the inset of Fig. 3. Figure 3 depicts the frequency of up to 29 eigenmodes of three SiN–FS string resonators. Solid lines represent fits of the string model ($f_n \approx (n/2L)\sqrt{\sigma/\rho}$) with σ being the only free parameter (see the supplementary material). The slight deviation observed for high mode numbers is a consequence of the bending contribution neglected in this approximation. Note the fit of the full model [Eq. (1)] yields a somewhat better agreement; however, Young's modulus cannot be reliably extracted as a second free parameter in the stress-dominated regime.

However, taking advantage of Eq. (3), we can now determine Young's modulus along with its uncertainty for each combination of n and m. All input parameters as well as their uncertainties are listed in the supplementary material. To get as much statistics as possible, we introduce the difference of two mode numbers $\Delta = |m - n|$ as a parameter. For instance, $\Delta = 5$ corresponds to the combinations $(n = 1, m = 6), 2, 7, 3, 8, \ldots,$. For each Δ, we calculate the mean value of $\bar{E}$ and $\overline{\delta E}$.

The obtained values of Young's modulus are depicted as a function of Δ for all four materials in Fig. 4. Note that only Δ values comprising two or more combinations of mode numbers are shown. The individual combinations $E(\Delta)$ contributing to $\bar{E}$ for a specific Δ are visualized as gray crosses, whereas the mean values of Young's modulus $\bar{E}$ for each value of Δ are included as colored circles.

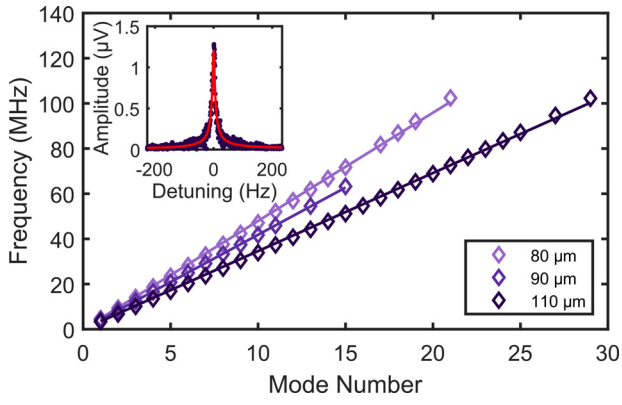

FIG. 3. Measured eigenfrequency as a function of the mode number for the three longest SiN-FS strings including fits of the string model (solid lines). Inset depicts the frequency response of the fundamental mode ($n = 1$, $L = 110\ \mu$m, $f_1 = 3.37$ MHz), including a Lorentzian fit (solid lines) to the data (dots).

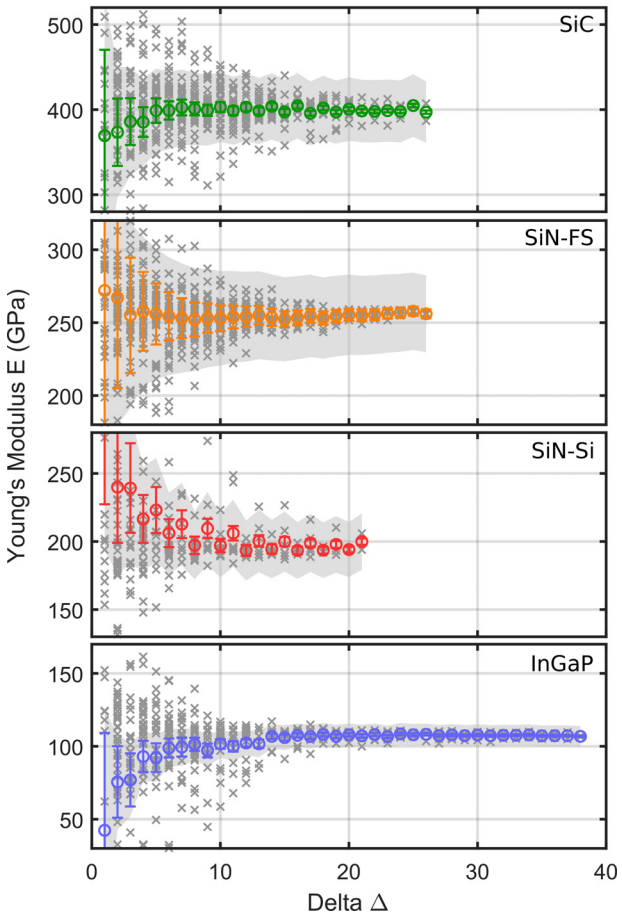

FIG. 4. Determined Young's modulus as a function of Δ for the four different materials SiC (green), SiN–FS (orange), SiN–Si (red), and InGaP (blue). Gray crosses correspond to individual combinations of $|m - n|$. Their mean values $\bar{E}(\Delta)$ are shown as colored circles. Note that while all combinations of n, m are included in the calculation of $\bar{E}$ for a given Δ, not all of them are shown as gray crosses as some heavy outliers appearing mostly for low values of Δ have been truncated for the sake of visibility. The complete uncertainty is represented by the gray shade, whereas its Δ-dependent contribution arising from the uncertainty in the eigenfrequency determination is represented by the colored error bars.

Clearly, Young's modulus of each material converges to a specific value for increasing Δ. These values are extracted by averaging over the obtained values of $\bar{E}$ and summarized in Table I. Note that only the upper half of the available Δ points have been included in the average in order to avoid some systematic distortions appearing for low Δ.

The uncertainty associated with the mean Young's modulus $\overline{\delta E}$ is indicated by gray shades. As discussed in more detail in the

TABLE I. Young's modulus including the total uncertainty determined for the four different materials.

	SiN–FS	SiN–Si	SiC	InGaP
E (GPa)	254(28)	198(22)	400(38)	108(7)

supplementary material, the Δ-dependence of the uncertainty arises solely from the uncertainty in the eigenfrequency determination. Therefore, this contribution to the total uncertainty is highlighted separately as colored error bars.

For small Δ, a large uncertainty in the eigenfrequency determination is observed, which dominates the complete uncertainty $\overline{\delta E}$. It coincides with a considerable scatter of the individual combinations, which is also attributed to the impact of the eigenfrequency determination. As expected, for increasing Δ, the uncertainty in the eigenfrequency determination decreases, such that the complete uncertainty $\overline{\delta E}$ becomes dominated by the constant contribution originating from the uncertainties in the density, thickness, and length of the string. The total uncertainty is obtained by averaging $\overline{\delta E}$ over the upper half of the available Δ points. It is also included in Table I.

The resulting values for Young's modulus are also included in Fig. 1 as colored dots using the same color code as in Fig. 4. Clearly, the determined values coincide with the parameter corridor suggested by our analysis of the literature: for InGaP, where no independent literature values are available, we compute Young's modulus[13] from the elastic constants of InGaP with the appropriate Ga content ($x = 0.585$) and crystal orientation [110], yielding $E^{\mathrm{th}}_{\mathrm{InGaP}} = 123$ GPa[13,43] (which is included as the theory value for InGaP in Fig. 4). This is rather close to our experimentally determined value of $E_{\mathrm{InGaP}} = 108 \pm 7$ GPa. For SiC, we can calculate Young's modulus as well; however, the elastic constants required for the calculations vary dramatically in the literature. As also included as theory values in Fig. 1, we can produce values of $E^{\mathrm{th}}_{\mathrm{SiC}} = 125$,[14] 286,[36] 419,[37] 452,[38] or 466 GPa,[15] just by choosing different references for the elastic constants. For our material, we measure a Young's modulus of $E_{\mathrm{SiC}} = 400 \pm 38$ GPa, which is in perfect agreement with the experimentally determined literature values of 398[22] and 400 GPa[18] by Iacopi *et al.* It is also in good agreement with the elastic constants published by Li and Bradt,[37] yielding 419 GPa for the orientation of our string resonators. Interestingly, SiN –FS and SiN –Si exhibit significantly different Young's moduli of $E_{\mathrm{SiN-FS}} = 254 \pm 28$ and $E_{\mathrm{SiN-Si}} = 198 \pm 22$ GPa, respectively. In Fig. 1, we can see two small clusters of measured Young's moduli around our determined values, suggesting that the exact Young's modulus depends on growth conditions and the subjacent substrate material even for the case of an amorphous resonator material.

In conclusion, we have presented a thorough analysis of Young's modulus of strongly stressed nanostring resonators fabricated from four different wafer materials. The demonstrated method to extract Young's modulus yields an accurate prediction with well-defined uncertainty. It is suitable for all types of nano- or micromechanical resonators subjected to intrinsic tensile stress. As we also show that literature values provide hardly the required level of accuracy for quantitative analysis, even when considering the appropriate material specifications, the *in situ* determination of Young's modulus is an indispensable tool for the precise and complete sample characterization, which can significantly improve the design of nanomechanical devices to fulfill quantitative specifications or the comparison of experimental data to quantitative models when not using free fitting parameters. Furthermore, the presented strategy can also be applied to two-dimensional tensioned membrane resonators. However, in the case of anisotropic Young's modulus, only an average value will be accessible, such that the present case of a one-dimensional string resonator is better suited to characterize Young's modulus of a crystalline resonator.

See the supplementary material for a list of used material parameters, a discussion of the uncertainties, and the stress dependence of Young's modulus.

The authors acknowledge the financial support from the European Unions Horizon 2020 program for Research and Innovation under Grant Agreement No. 732894 (FET Proactive HOT) and the German Federal Ministry of Education and Research through Contract No. 13N14777 funded within the European QuantERA cofund project QuaSeRT. We further acknowledge financial support from the Deutsche Forschungsgemeinschaft (DFG, German Research Foundation) through Project-ID 425217212 - SFB 1432 and via Project No. WE 4721/1-1 as well as project QT-6 SPOC of the Baden-Württemberg Foundation.

AUTHOR DECLARATIONS

Conflict of Interest

The authors have no conflicts to disclose.

Author Contributions

Yannick Klaß: Data curation (supporting); Investigation (lead); Visualization (lead); Writing – original draft (lead); Writing – review and editing (lead). **Juliane Doster:** Conceptualization (supporting); Investigation (supporting); Writing – review and editing (supporting). **Maximilian Bückle:** Investigation (supporting); Writing – review and editing (supporting). **Remy Braive:** Resources (supporting). **Eva Maria Weig:** Conceptualization (supporting); Funding acquisition (lead); Resources (lead); Visualization (supporting); Writing – review and editing (supporting).

DATA AVAILABILITY

The data that support the findings of this study are openly available in Zenodo at http://doi.org/10.5281/zenodo.6951670, Ref. 44.

REFERENCES

[1]A. Bachtold, J. Moser, and M. Dykman, "Mesoscopic physics of nanomechanical systems," arXiv:2202.01819 (2022).
[2]M. Aspelmeyer, T. J. Kippenberg, and F. Marquardt, "Cavity optomechanics," Rev. Mod. Phys. **86**, 1391 (2014).
[3]P. Delsing, A. N. Cleland, M. J. Schuetz, J. Knörzer, G. Giedke, J. I. Cirac, K. Srinivasan, M. Wu, K. C. Balram, C. Bäuerle *et al.*, "The 2019 surface acoustic waves roadmap," J. Phys. D **52**, 353001 (2019).
[4]A. Clerk, K. Lehnert, P. Bertet, J. Petta, and Y. Nakamura, "Hybrid quantum systems with circuit quantum electrodynamics," Nat. Phys. **16**, 257 (2020).
[5]S. Volz, J. Ordonez-Miranda, A. Shchepetov, M. Prunnila, J. Ahopelto, T. Pezeril, G. Vaudel, V. Gusev, P. Ruello, E. M. Weig *et al.*, "Nanophononics: State of the art and perspectives," Eur. Phys. J. B **89**(1), 15 (2016).
[6]M. Perdriat, C. Pellet-Mary, P. Huillery, L. Rondin, and G. Hétet, "Spin-mechanics with nitrogen-vacancy centers and trapped particles," Micromachines **12**, 651 (2021).
[7]B. Hähnlein, M. Stubenrauch, S. Michael, and J. Pezoldt, "Mechanical properties and residual stress of thin 3C-SiC (111) films determined using mems structures," Mater. Sci. Forum **778–780**, 444–448 (2014).
[8]B. Hähnlein, M. Stubenrauch, and J. Pezoldt, "Mechanical properties and residual stress of thin 3C-SiC (100) films determined using mems structures," Mater. Sci. Forum **821–823**, 281–284 (2015).

[9]K. Babaei Gavan, H. J. Westra, E. W. van der Drift, W. J. Venstra, and H. S. van der Zant, "Size-dependent effective Young's modulus of silicon nitride cantilevers," Appl. Phys. Lett. **94**, 233108 (2009).
[10]V. Kulikovsky, V. Vorlíček, P. Boháč, M. Stranyánek, R. Čtvrtlík, A. Kurdyumov, and L. Jastrabik, "Hardness and elastic modulus of amorphous and nanocrystalline SiC and Si films," Surf. Coat. Technol. **202**, 1738 (2008).
[11]Q. P. Unterreithmeier, T. Faust, and J. P. Kotthaus, "Damping of nanomechanical resonators," Phys. Rev. Lett. **105**, 027205 (2010).
[12]T. Yoshioka, T. Ando, M. Shikida, and K. Sato, "Tensile testing of SiO_2 and Si_3N_4 films carried out on a silicon chip," Sens. Actuators, A **82**, 291 (2000).
[13]M. Bückle, V. C. Hauber, G. D. Cole, C. Gärtner, U. Zeimer, J. Grenzer, and E. M. Weig, "Stress control of tensile-strained $In_{1-x}Ga_xP$ nanomechanical string resonators," Appl. Phys. Lett. **113**, 201903 (2018).
[14]R. J. Meyer and L. Gmelin, *Gmelins Handbuch Der Anorganischen Chemie* (Verlag Chemie GmbH, Weinheim, 1926).
[15]K. Karch, P. Pavone, W. Windl, O. Schütt, and D. Strauch, "Ab initio calculation of structural and lattice-dynamical properties of silicon carbide," Phys. Rev. B **50**, 17054 (1994).
[16]H. Guo and A. Lal, "Characterization of micromachined silicon nitride membrane using resonant ultrasound spectroscopy," in *IEEE Ultrasonics Symposium. Proceedings. An International Symposium (Cat. No. 01CH37263)*, Vol. 2 (IEEE, 2001), pp. 863–866.
[17]D. Schneider and M. Tucker, "Non-destructive characterization and evaluation of thin films by laser-induced ultrasonic surface waves," Thin Solid Films **290–291**, 305 (1996).
[18]F. Iacopi, G. Walker, L. Wang, L. Malesys, S. Ma, B. V. Cunning, and A. Iacopi, "Orientation-dependent stress relaxation in hetero-epitaxial 3C-SiC films," Appl. Phys. Lett. **102**, 011908 (2013).
[19]T.-Y. Zhang, Y.-J. Su, C.-F. Qian, M.-H. Zhao, and L.-Q. Chen, "Microbridge testing of silicon nitride thin films deposited on silicon wafers," Acta Mater. **48**, 2843 (2000).
[20]R. Edwards, G. Coles, and W. Sharpe, "Comparison of tensile and bulge tests for thin-film silicon nitride," Exp. Mech. **44**, 49 (2004).
[21]O. Tabata, K. Kawahata, S. Sugiyama, and I. Igarashi, "Mechanical property measurements of thin films using load-deflection of composite rectangular membranes," Sens. Actuators **20**, 135 (1989).
[22]F. Iacopi, R. E. Brock, A. Iacopi, L. Hold, and R. H. Dauskardt, "Evidence of a highly compressed nanolayer at the epitaxial silicon carbide interface with silicon," Acta Mater. **61**, 6533 (2013).
[23]W.-H. Chuang, T. Luger, R. K. Fettig, and R. Ghodssi, "Mechanical property characterization of lpcvd silicon nitride thin films at cryogenic temperatures," J. Microelectromech. Syst. **13**, 870 (2004).
[24]S. Schmid, K. Jensen, K. Nielsen, and A. Boisen, "Damping mechanisms in high-Q micro and nanomechanical string resonators," Phys. Rev. B **84**, 165307 (2011).
[25]S. S. Verbridge, J. M. Parpia, R. B. Reichenbach, L. M. Bellan, and H. G. Craighead, "High quality factor resonance at room temperature with nanostrings under high tensile stress," J. Appl. Phys. **99**, 124304 (2006).
[26]G. D. Cole, P.-L. Yu, C. Gärtner, K. Siquans, R. Moghadas Nia, J. Schmöle, J. Hoelscher-Obermaier, T. P. Purdy, W. Wieczorek, C. A. Regal, and M. Aspelmeyer, "Tensile-strained $In_xGa_{1-x}P$ membranes for cavity optomechanics," Appl. Phys. Lett. **104**, 201908 (2014).
[27]A. R. Kermany, G. Brawley, N. Mishra, E. Sheridan, W. P. Bowen, and F. Iacopi, "Microresonators with Q-factors over a million from highly stressed epitaxial silicon carbide on silicon," Appl. Phys. Lett. **104**, 081901 (2014).
[28]G. I. González and P. R. Saulson, "Brownian motion of a mass suspended by an anelastic wire," J. Acoust. Soc. Am. **96**, 207 (1994).
[29]P.-L. Yu, T. P. Purdy, and C. A. Regal, "Control of material damping in high-Q membrane microresonators," Phys. Rev. Lett. **108**, 083603 (2012).
[30]Y. Tsaturyan, A. Barg, E. S. Polzik, and A. Schliesser, "Ultracoherent nanomechanical resonators via soft clamping and dissipation dilution," Nat. Nanotechnol. **12**, 776 (2017).
[31]A. H. Ghadimi, S. A. Fedorov, N. J. Engelsen, M. J. Bereyhi, R. Schilling, D. J. Wilson, and T. J. Kippenberg, "Elastic strain engineering for ultralow mechanical dissipation," Science **360**, 764 (2018).
[32]O. Maillet, X. Zhou, R. Gazizulin, A. M. Cid, M. Defoort, O. Bourgeois, and E. Collin, "Nonlinear frequency transduction of nanomechanical Brownian motion," Phys. Rev. B **96**, 165434 (2017).
[33]L. G. Villanueva and S. Schmid, "Evidence of surface loss as ubiquitous limiting damping mechanism in SiN micro-and nanomechanical resonators," Phys. Rev. Lett. **113**, 227201 (2014).
[34]P. Sadeghi, M. Tanzer, S. L. Christensen, and S. Schmid, "Influence of clamp-widening on the quality factor of nanomechanical silicon nitride resonators," J. Appl. Phys. **126**, 165108 (2019).
[35]J. Chan, M. Eichenfield, R. Camacho, and O. Painter, "Optical and mechanical design of a 'zipper' photonic crystal optomechanical cavity," Opt. Express **17**, 3802 (2009).
[36]I. K. A. Pestka, J. Maynard, D. Gao, and C. Carraro, "Measurement of the elastic constants of a columnar sic thin film," Phys. Rev. Lett. **100**, 055503 (2008).
[37]Z. Li and R. C. Bradt, "The single-crystal elastic constants of cubic (3C) SiC to 1000° C," J. Mater. Sci. **22**, 2557 (1987).
[38]C.-Z. Wang, R. Yu, and H. Krakauer, "Pressure dependence of born effective charges, dielectric constant, and lattice dynamics in SiC," Phys. Rev. B **53**, 5430 (1996).
[39]W. Weaver, Jr., S. P. Timoshenko, and D. H. Young, *Vibration Problems in Engineering* (Wiley, New York, 1990).
[40]A. N. Cleland, *Foundations of Nanomechanics: From Solid-State Theory to Device Applications* (Springer, Berlin, 2002).
[41]M. Bückle, Y. S. Klaß, F. B. Nägele, R. Braive, and E. M. Weig, "Universal length dependence of tensile stress in nanomechanical string resonators," Phys. Rev. Appl. **15**, 034063 (2021).
[42]S. Hong, T. Weihs, J. Bravman, and W. Nix, "Measuring stiffnesses and residual stresses of silicon nitride thin films," J. Electron. Mater. **19**, 903 (1990).
[43]M. S. Shur, M. Levinshtein, and S. Rumyantsev, *Handbook Series on Semiconductor Parameters*, Ternary and Quaternary III–V Compounds Vol. 2 (World Scientific Publishing Co, Singapore, 1999). See also: http://www.ioffe.ru/SVA/NSM/
[44]Y. S. Klaß, J. Doster, M. Bückle, R. Braive, and E. M. Weig, "Determining Young's modulus via the eigenmode spectrum of a nanomechanical string resonator," Zenodo (2022).